Journal of Dental Sciences 19 (2024) 2140–2149

Available online at www.sciencedirect.com

ScienceDirect

journal homepage: www.e-jds.com

Original Article

Personalized prosthesis design in all-on-4® treatment through deep learning-accelerated structural optimization

Yung-Chung Chen [a,b], Kuan-Hsin Wang [c], Chi-Lun Lin [c,d*]

[a] School of Dentistry & Institute of Oral Medicine, College of Medicine, National Cheng Kung University, Tainan, Taiwan
[b] Division of Prosthodontics, Department of Stomatology, National Cheng Kung University Hospital, College of Medicine, National Cheng Kung University, Tainan, Taiwan
[c] Department of Mechanical Engineering, National Cheng Kung University, Tainan, Taiwan
[d] Medical Device Innovation Center, National Cheng Kung University, Tainan, Taiwan

Received 4 March 2024; Final revision received 15 March 2024
Available online 27 March 2024

KEYWORDS
Dental implantation;
Finite element analysis;
Machine learning;
Dental prothesis design

Abstract *Background/purpose:* The All-on-4® treatment concept is a dental procedure that utilizes only four dental implants to support a fixed prosthesis, providing full-arch rehabilitation with affordable cost and speedy treatment courses. Although the placement of all-on-4® implants has been researched in the past, little attention was paid to the structural design of the prosthetic framework.
Materials and methods: This research proposed a new approach to optimize the structure of denture framework called BESO-Net, which is a bidirectional evolutionary structural optimization (BESO) based convolutional neural network (CNN). The approach aimed to reduce the use of material for the framework, such as Ti–6Al–4V, while maintaining structural strength. The BESO-Net was designed as a one-dimensional CNN based on Inception V3, trained using finite element analysis (FEA) data from 14,994 design configurations, and evaluated its training performance, generalization capability, and computation efficiency.
Results: The results suggested that BESO-Net accurately predicted the optimal structure of the denture framework in various mandibles with different implant and load settings. The average error was found to be 0.29% for compliance and 11.26% for shape error when compared to the traditional BESO combined with FEA. Additionally, the computational time required for structural optimization was significantly reduced from 6.5 h to 45 s.

* Corresponding author. Department of Mechanical Engineering, National Cheng Kung University, 1 University Road, Tainan 70160, Taiwan.
E-mail address: linc@ncku.edu.tw (C.-L. Lin).

https://doi.org/10.1016/j.jds.2024.03.017

Conclusion: The proposed approach demonstrates its applicability in clinical settings to quickly find personalized All-on-4® framework structure that can significantly reduce material consumption while maintaining sufficient stiffness.

Introduction

The All-on-4® treatment concept is a method of restoring a full arch of teeth for edentulous patients.[1] This method makes the most of the remaining bone in patients with atrophic jaws, allowing immediate functionality without additional procedures. However, the decision-making process for implant placement is often based on the clinician's experience rather than a thorough evaluation of the biomechanics involved.[2,3]

Assessing the biomechanical performance of the peri-implant bone is critical to the success of a treatment plan. Finite element analysis can simulate the biomechanical behavior between the implant and jawbone before surgery and provide valuable information for treatment planning.[4] Additionally, optimization techniques can be used with finite element analysis to find a biomechanically optimized all-on-4® configuration based on patient-specific conditions, thereby improving post-operative stability and reducing the risk of complications.[5] An integration of these engineering techniques can be a useful tool to provide valuable insights and assist clinicians in making a more informed decision for the treatment.

When planning an all-on-4® treatment, it is important to consider both the placement of implants and the design of the prosthetic framework. While the former has been extensively discussed in literature,[4,6—13] the latter has received less attention.

Topology optimization is a technique often used in structural engineering to find the optimal shape of a structure while adhering to specific constraints, loads, and target volumes. This method helps minimize material usage while still maintaining desired structural stiffness. Recently, topology optimization has also been applied in dentistry to optimize dental prosthesis and implant designs. By combining finite element analysis (FEA) and topology optimization techniques, it is possible to improve the structural performance of dental prosthetics and implants in the surrounding bone.[14—17] FEA provides accurate simulations of complex mechanical behavior for the calculation of objective function. However, the computation cost associated with this combined method can be prohibitive, making it difficult to use for real-time clinical decision support.

A machine learning or deep learning model can be trained to replace the role of FEA in an optimization process. Artificial neural networks (ANNs) are advanced computational models that take inspiration from the structure and functionality of human brains. They are composed of interconnected nodes that work together to simulate the learning and decision-making processes observed in biological systems. ANNs gained popularity in the late 1980s with the rediscovery of back-propagation algorithms, which are highly regarded for their ability to recognize patterns and generalize. ANNs are superior to logistic regression in modeling complex nonlinear relationships and have advanced to meet challenges beyond traditional statistical methods, such as computer vision and speech recognition. Some studies have successfully trained ANNs to predict the objective function, saving computation costs in every optimization iteration.[18—21]

Convolutional Neural Networks (CNNs) are a type of deep neural network that excel in processing structured grid data, such as images, due to their unique architecture inspired by the human visual system. Through the use of convolution and pooling layers, CNNs can automatically identify and learn spatial feature hierarchies, ranging from simple edges to complex objects. This remarkable ability has revolutionized the field of computer vision and led to breakthroughs in image and video recognition, medical image analysis, image classification, and autonomous driving systems. CNNs have also been implemented to speed up traditional topology optimization methods.[22—30] For instance, Lee et al. proposed the use of a FEA-based CNN for fast prediction of compliances for topology optimization,[30] while Xiang et al. presented a CNN-based approach for 3D structural optimization, allowing direct prediction of optimal structures without the need for iterative processes. These studies show the potential of machine learning techniques in finding optimal structural designs. However, the designs shown in these studies were simple 2D or 3D cantilever structures. For structural optimization of an all-on-4® prosthetic framework, more advanced techniques are needed to overcome challenges such as irregular jawbone geometries and interactions between multiple parts, which increase the complexity of the finite element model.

In this paper, we introduce a novel method that optimizes the structure of an All-on-4® prosthetic framework using CNN and bidirectional evolutionary structural optimization (BESO).[31] Firstly, we created an FEA model that reflects the use conditions of the All-on-4® treatment on a realistic jawbone. Then, we developed an automated process for generating FEA data and trained a CNN to perform non-iterative structural optimization. Finally, we evaluated the proposed method for its accuracy, versatility, and efficiency. Our approach can assist dental professionals in making informed decisions during the planning stage of All-on-4® treatment based on biomechanical considerations.

Materials and methods

Workflow of this study

We have developed a deep learning model called BESO-Net, which enables the prediction of the optimal structure of an all-on-4® prosthetic framework given the jawbone and implant placement without going through the iterative evolution process.

The development was divided into three stages. First, we created an FEA model using ABAQUS 2017 (Dassault Systems, Johnston, RI, USA) to simulate the biomechanical behavior of an all-on-4® treatment plan. The BESO was performed to iteratively run instances of FEA, and output data fields of FEA were collected to train a CNN (i.e., BESO-Net). Given a set of design parameters, the trained BESO-Net would be able predict the optimal shape of a prosthetic framework. Finally, we evaluated the performance of BESO-Net by comparing its results with the traditional BESO process in terms of prediction accuracy and generalization capability. A complete flowchart of this study is shown in Fig. 1.

All the computation required for running simulations and CNN model training was performed on a workstation PC with an Intel Xeon W-2223 CPU at 3.60 GHz, an NVIDIA Quadro RTX4000 with 8 GB GPU, and 64 GB of memory.

Finite element modeling

A standard mandible model (SMM) was reconstructed based on a series of CBCT images from a subject (IRB No. A-ER-110-003) and further processed using Geomagic Studio 12 (3D Systems, Morrisville, NC, USA) to repair geometry and smoothen the surfaces to ensure the success of meshing in FEA. The SMM model was used as a baseline to create variations by adjusting the heights of different alveolar ridges, resulting another five types of mandibular models, including mesial-side high (MH), distal-side high (DH), right-side high (RH), left-side high (LH), and mesial-side low (ML), as shown in Fig. 2.

The implant design was based on the multi-unit abutment (Nobel Biocare, Kloten Switzerland) widely used in the All-on-4® treatment. The geometric parameters of the implants included length (l), diameter (d), and tangent inclination angle (ϕ_T), as shown in Fig. 3A. To facilitate the FEA, the 3D mandibular model underwent surface smoothing, crack repair, and geometric simplification. A coordinate system was defined by aligning the XY plane with the occlusal plane (Fig. 3B), and twelve points were then manually selected on the alveolar ridge surface to fit a curve of the arc, which allows the implants to be placed on. The angular position of an implant on the arc can be denoted by θ.

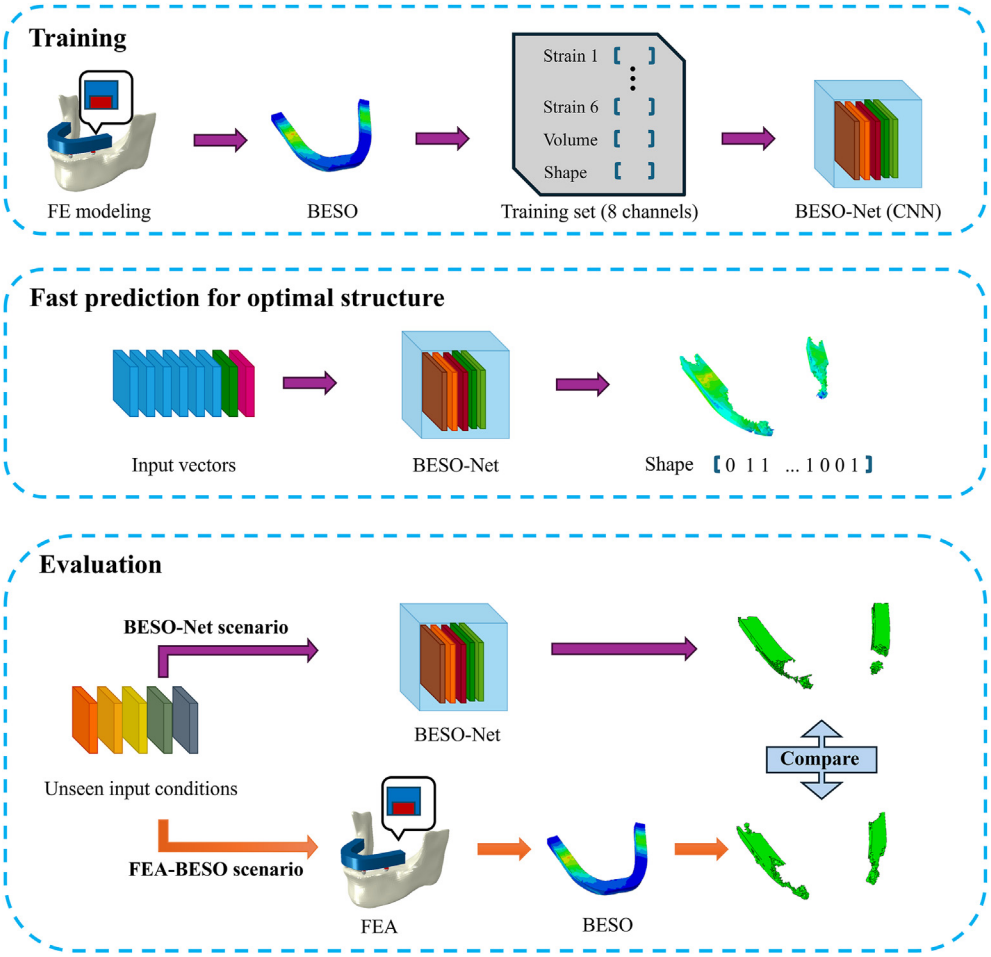

Figure 1 Flowchart of proposed approach. BESO: bidirectional evolutionary structural optimization. FEA: finite element analysis.

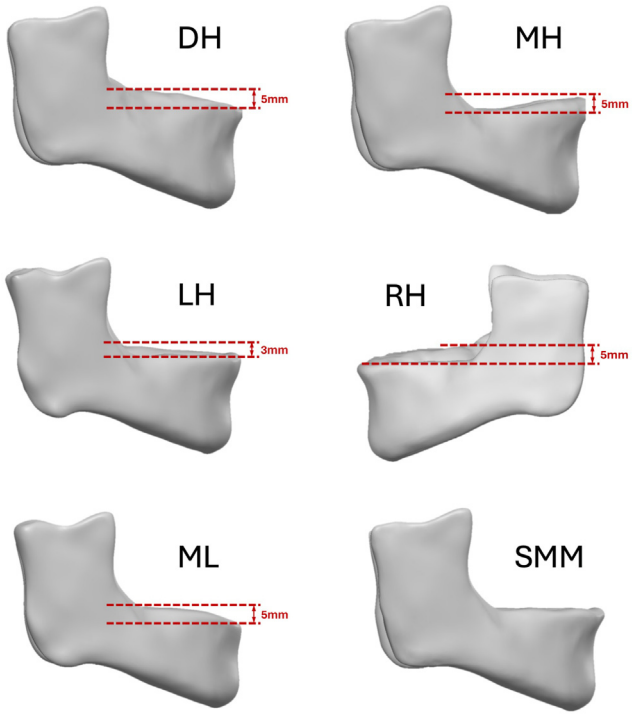

Figure 2 Standard mandibular model (SMM) and five modified types, which are mesial-side high (MH), distal-side high (DH), right-side high (RH), left-side high (LH), and mesial-side low (ML).

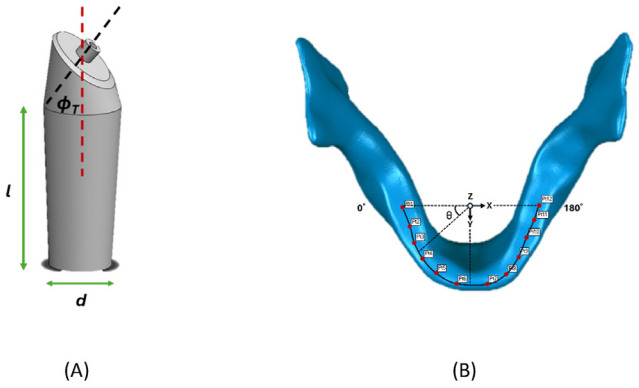

(A) (B)

Figure 3 Design parameters of implants (A) and angular position (θ) of implant placement on jawbone (B).

The initial structure of the prosthetic framework was constructed in two steps, as shown in Fig. 4. First, four implants and abutment teeth were created and positioned according to input implant parameters. A 6 mm × 4 mm titanium alloy prosthetic framework (red region) was then generated on top of the four implants. Next, a layer of PEEK material is extended 6 mm upward and 2 mm on each side of the framework to simulate the prosthetic crowns (blue region). The volume of the prosthetic framework was defined as the design region, where material substitutions were allowed during the evolutionary optimization process of BESO.

The region 38 mm above the occlusal plane of the mandible model, corresponding to the condylar region, was

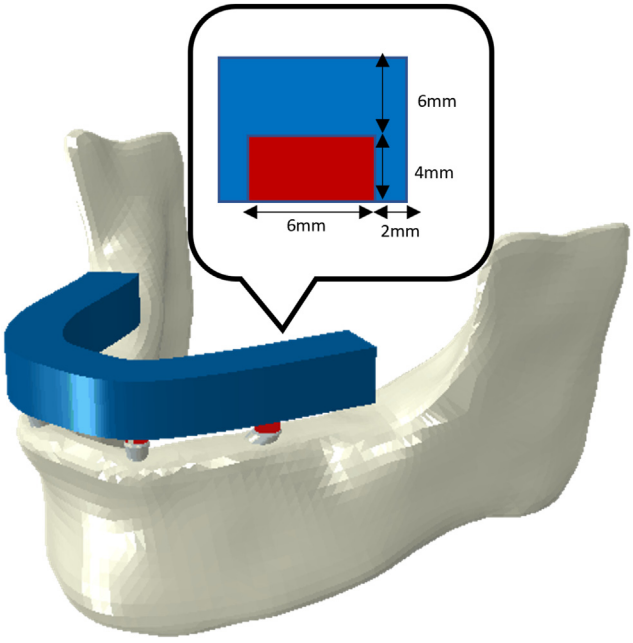

Figure 4 Assembled geometric model that includes jawbone, four implants, and framework structure with titanium alloy prosthetic framework as design region (in red) and prosthetic crown as non-design region (in blue). (For interpretation of the references to color in this figure legend, the reader is referred to the Web version of this article).

fully fixed to mimic the stabilizing effect of the TMJ. To account for incomplete bone integration after implantation, the contact between the implants and the bone was modeled with friction ($\mu = 0.3$). The interface between the prosthetic framework and implants was fully bonded. A load condition based on previous research was used to simulate maximum occlusal forces.[32] Therefore, pressure loads of 525 N, 110 N, and 120 N were applied to the locations of posterior molars, premolars, and anterior teeth over circular areas with radii of 2.1 mm, 1 mm, and 1.1 mm, respectively (Fig. 5).

All materials were assumed to be homogeneous and isotropic. The prosthetic framework were composed of titanium alloy (Ti–6Al–4V) and polyetheretherketone (PEEK), while the implants were made of titanium alloy. The mandible was represented as a composite structure consisting of the outer cortical bone and the inner cancellous bone. The material properties of all parts are listed in Table 1. The model was meshed using C3D4 elements, a convergence study was conducted to assign the mesh size of mandible as 2 mm, peri-implants area as 0.25 mm, and prosthetic framework as 1 mm, resulting in 523,647 elements and 199,925 nodes.

Bidirectional evolutionary structural optimization algorithm

BESO iteratively analyzes the sensitivity of finite elements and determines whether to retain or replace them in order to minimize the average compliance of the structure, which can be expressed mathematically as follows.[33]

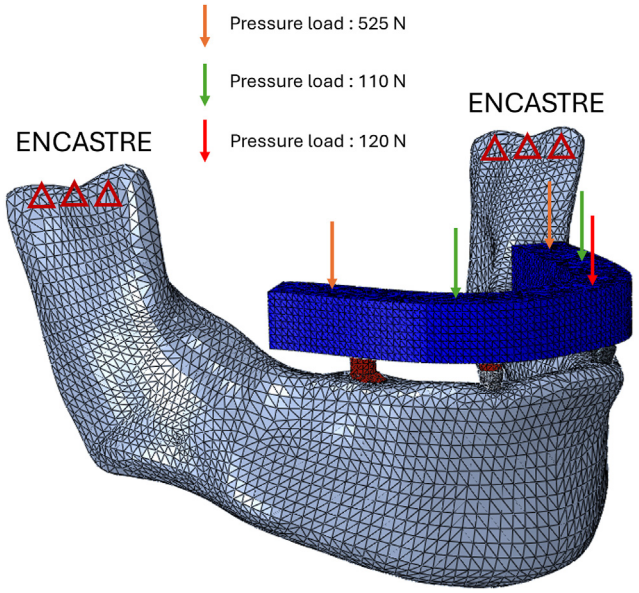

Figure 5 Finite element model with specified boundary condition and loading.

Table 1 Material properties.

Material	Young's modulus (MPa)	Poisson's ratio
Cortical bone	14,000	0.3
Trabecular bone	1400	0.3
Ti—6Al—4V	110,000	0.35
Polyetheretherketone (PEEK)	3000	0.36

$$minimize: C = \frac{1}{2}\boldsymbol{u}^T\boldsymbol{K}\boldsymbol{u} \quad \text{Eq1}$$

$$Subject\ to: V^* - \sum_{i=1}^{N} V_i x_i = 0 \quad \text{Eq2}$$

$$x_i = x_{min}\ or\ 1 \quad \text{Eq3}$$

where C represents the objective function, which is the average compliance of the structure. $\boldsymbol{K}$ is the global stiffness matrix, $\boldsymbol{u}$ is the displacement vector, V_i is the volume of a single element, and V^* is the predetermined volume of the structure, known as the volume fraction. The parameter N denotes the total number of elements in the structure, while the design variable x_i denotes the relative density of the ith element. Setting x_i to 1 indicates a solid element, while x_{min} typically represents the density of a void element and is set to 0.001.

This study considered two non-void materials, and the material interpolation was performed using Eq. (4), where E_1 and E_2 represent the Young's moduli of the two materials, and p denotes the penalty exponent, which is usually set to 3. It is important to note that $E_1 > E_2 \neq 0$. The calculation of the element sensitivity (α_i) is formulated as Eq. (5).

$$E(x_i) = x_i^p E_1 + (1 - x_i^p) E_2 \quad \text{Eq4}$$

$$\alpha_i = \begin{cases} \frac{1}{2}\left[1 - \frac{E_2}{E_1}\right] u_i^T K_i u_i & for\ matreial\ 1 \\ \frac{1}{2}\frac{x_{min}^{p-1}(E_1 - E_2)}{x_{min}^p E_1 + (1 - x_{min}^p) E_2} u_i^T K_i u_i & for\ matreial\ 2 \end{cases} \quad \text{Eq5}$$

We developed ABAQUS Python scripts to automatically configure the FEA model's boundary conditions, loads, material properties, and meshing. By manually importing the jawbone model and assigning the implant design parameters, the required finite element models were created. Based on a basic BESO program,[34] we developed new ABAQUS Python scripts specifically for BESO optimization in the context of dental implant abutment design. These scripts required only the input of the target volume, material properties, volume fraction evolution rate, and convergence criteria to automatically initiate the BESO optimization process.

Development of bidirectional evolutionary structural optimization neural network

We modified the model architecture based on the Inception V3 network to create a one-dimensional CNN,[35] as shown in Table 2. The Adaptive Moment Estimation (ADAM) optimizer was used, and the loss function was binary cross-entropy because the model output is composed of 0s and 1s to represent the shape matrix of the support structure. The batch size was set as eight, and dropout and early stopping techniques were incorporated to improve the generalization ability of the model. The hyperparameters were summarized in Table 3.

The input of BESO-Net had eight channels including tensile strain (in x, y, and z directions), shear strain (in x, y, and z directions), initial shape of the framework structure, and difference in volume fraction. Each channel was in the form of 1-dimensional matrices with a length equal to the number of elements.

The training set involved four types of jawbone (SMM, DH, MH, and RH) configured with three random implant

Table 2 Architecture of BESO-Net.

Type	Patch size/Stride	Input size
Convolution	3/2	25,000 × 8
Convolution	3/1	12,499 × 4
Conv padded	3/1	12,497 × 4
Pool	3/2	12,497 × 8
Convolution	3/1	6248 × 8
Convolution	3/2	6248 × 10
Convolution	3/1	6246 × 24
Inception	3 × Inception module	3122 × 24
Inception	3 × Inception module	1561 × 48
Inception	3 × Inception module	780 × 96
Pool	3	780 × 128
Flatten		128
Sigmoid	Classifier	25,000 × 1

BESO: bidirectional evolutionary structural optimization.

Table 3 Hyperparameters used to train BESO-Net.

Optimizer	
Optimizer	ADAM
Learning rate	0.0001
First moment estimate	0.9
Second moment estimate	0.999
Training	
Batch size	8
Epoch	1000
Early stopping patience	15
Early stopping monitor	Validation loss
Loss function	Binary cross entropy

BESO: bidirectional evolutionary structural optimization. ADAM: Adaptive Moment Estimation.

placements, resulting in 12 FEA model instances. FEA data was generated by performing BESO for each of these model instances with the target volume set from 0.8 to 0.4. Table 4 shows the amount of data collected at different values of target volume. During the training process, the data was randomly divided into a 70% training set and a 30% validation set. The performance of the BESO-Net was evaluated by the validation set to measure the effectiveness and accuracy of the training process.

The generalization test evaluated the BESO-Net's adaptability to three types of unseen conditions (jawbone, loading, and implant placement). First, the two jawbone models, LH and ML, which were not included in the training set, were used to test the BESO-NET. Secondly, the load changes were introduced to the SMM jawbone by modifying the two pressure loads applied at the areas of posterior molars from 525 to 50 N and the two applied at the areas of premolars from 110 to 55 N (Fig. 5), while the one applied at the area of anterior teeth was unchanged. The significant changes in loads were specified to ensure an effective generalization test, but not intended for matching particular settings found in the existing literature. Finally, new implant placements were tested on the SMM and DH jawbones. The optimal structures obtained by BESO-NET were compared with the results of BESO, which iteratively performed FEA and discovered the optimal design (FEA-BESO). The differences in shape and average compliance were calculated, where the shape error is the discrepancy in the number of elements preserved as hard material between the optimal designs found by BESO-NET and FEA-BESO divided by the total number of elements in the framework structure.

Table 4 Amount of data collected for training BESO-Net.

Target volume	Quantity of data
0.4	5760
0.5	4137
0.6	2606
0.7	1520
0.8	971

BESO: bidirectional evolutionary structural optimization.

Results

The training process of BESO-Net reached convergence at epoch 83 when the loss was 0.1279 (Fig. 6). The early stopping mechanism terminated the training at epoch 98 because the validation loss of did not decrease for 15 epochs. The total training time was 19.6 min.

During the testing phase, BESO-Net was evaluated on five test cases which included two jawbones (LH and ML) that were unseen, new implant placements on SMM and DH jawbones, and modified load conditions (on SMM). The results showed that the errors in compliance between BESO-Net and FEA-BESO were within 2% and the shape errors ranged from 4.22% to 17.55% (Table 5). Furthermore, the compliance of the optimal structure predicted by BESO-Net demonstrated the same trend as the FEA-BESO results in response to the target volume change.

When the target volume was greater than 0.6 (40% reduction in material), both methods achieved the goal without significantly affecting the compliance of the structure. This means that the compliance was similar to the initial structure (values in the column of target volume = 1). However, when the target volume was set to 0.5 or lower (more than 50% material reduction), the compliance of the structure slightly increased, indicating that the structural strength would not be maintained at the same level as the initial design.

This study assessed the accuracy of the BESO-Net in predicting the optimal shape of a framework by comparing it with FEA-BESO. The evaluation was based on the difference between the optimal shapes obtained by both methods, which included the incorrect assignment of a hard material element as a soft one, and vice versa. The BESO-Net still showed an 88.7% accuracy rate in predicting the optimal shape using this more comprehensive calculation of error. Results showed that the prediction accuracy was higher when the target volume was set at a mid-level range of 0.6–0.7, but less accurate when the target volume was set at low or high levels.

The optimized structures for the five scenarios are depicted in Fig. 7, which shows only the preserved hard

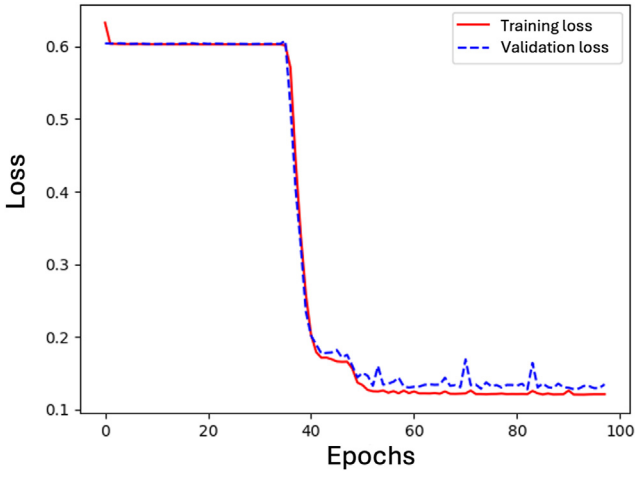

Figure 6 Loss evaluated on training and validation set during training process.

Table 5 Results of the five generalization test cases, including two unseen jawbones, left-side high (LH) and mesial-side low (ML) models (#1 & #2), new implant placements on standard mandibular model (SMM) and distal-side high (DH) jawbones (#3 & #4), and modified load conditions (#5). Unit of compliance is N·mm.

Case	Result item		Target volume						
			1	0.9	0.8	0.7	0.6	0.5	0.4
1	Compliance	FEA-BESO	512.7	512.8	513.4	514.9	517.2	521.9	529.6
		BESO-Net	512.7	517.3	513.7	515.6	518.4	522.5	529.2
		Error (%)	—	0.87	0.06	0.14	0.22	0.11	0.08
	Shape difference	# of elements	0	3929	1281	2052	2649	3005	3364
		Error (%)		17.9	5.84	9.35	12.07	13.69	15.32
2	Compliance	FEA-BESO	411.8	412.1	413.1	415.2	418.3	423.5	432.8
		BESO-Net	411.8	416.5	413.4	415.7	419.7	425.1	433.2
		Error (%)	—	1.07	0.09	0.12	0.33	0.37	0.07
	Shape difference	# of elements	0	3549	1609	2399	2754	3200	3228
		Error (%)		17.55	7.96	11.86	13.62	15.82	15.96
3	Compliance	FEA-BESO	305.9	306.1	306.5	307.6	309.6	314	322.8
		BESO-Net	305.9	306	306.7	307.7	309.8	314.7	323.9
		Error (%)	—	0.01	0.01	0.01	0.06	0.2	0.35
	Shape difference	# of elements	0	992	1295	1631	1868	2419	2757
		Error (%)		4.38	5.72	7.21	8.26	10.69	12.19
4	Compliance	FEA-BESO	263.3	263.4	263.8	264.9	267	271.9	281
		BESO-Net	263.3	268.5	263.9	265	267.6	273.8	284.4
		Error (%)	—	1.93	0.03	0.04	0.2	0.68	1.21
	Shape difference	# of elements	0	3954	982	1520	1928	2405	2836
		Error (%)		17.01	4.22	6.54	8.29	10.35	12.2
5	Compliance	FEA-BESO	25.5	25.5	25.6	25.6	25.6	25.7	25.9
		BESO-Net	25.5	25.6	25.6	25.6	25.6	25.7	25.9
		Error (%)	—	0.23	0.01	0	0.04	0.1	0.12
	Shape difference	# of elements	0	3919	1299	2104	2712	3103	3418
		Error (%)		17.46	5.79	9.37	12.08	13.82	15.23

material elements. It is evident that both methods retained the hard material in comparable regions for the optimal structure. However, the LH and ML cases exhibited more apparent shape errors, which we will discuss in a later section.

Compared with FEA-BESO, the computation efficiency of BESO-Net was significantly superior. With the target volume set to 0.4, FEA-BESO performed 55 iterations to converge to the optimum, which required approximately 6 h and 35 min of computing time. For the same setting, BESO-Net required no iteration and directly predicted the optimum in 45 s.

Discussion

The BESO-Net training set primarily consisted of FEA data, and its output shape data requires importing to an FEA software program for post-analysis. To facilitate data conversion between the BESO-Net and FEA processes, we proposed using one-dimensional matrices as the input and output data format. However, in more complex models, these matrices may contain a very long sequence of data, which could hinder the CNN's ability to capture long-range dependencies in the dataset due to the fixed size of the convolutional kernels. This limitation might have led to discrepancies in shape at the right side of the anterior teeth area for the LH and ML models (Fig. 7), where FEA-BESO completely replaced the hard materials, but BESO-Net preserved some hard material fragments. In the future, research could develop methods that transform the data into three-dimensional matrices and use a three-dimensional CNN architecture to train the model and address this limitation. However, the development of such a method should also consider the efficiency of data conversion between CNN and FEA.

This study selected two types of FEA output fields, which were tensile and shear strains, to train the BESO-Net and obtained satisfactory prediction results. However, it is important to recognize that other factors such as stress and displacement should also be considered in structural optimization. By examining the strain distribution in the material (Fig. 8), it is evident that BESO-Net tends to replace elements with lower strain values. For future studies, incorporating additional types of FEA data should be considered to enhance the model's accuracy. However, challenges associated with inconsistent data lengths and increased data size would need to be addressed during training.

This study has some limitations that need to be considered. Firstly, the SMM model was a simplified jawbone (e.g., the condyle region), and the other variations with adjusted height on one side were produced. Therefore, these models may not fully represent the different jawbone morphologies found in real patients. Additionally, the implant's geometry was simplified by only maintaining primary design parameters, and eliminating the threads. This

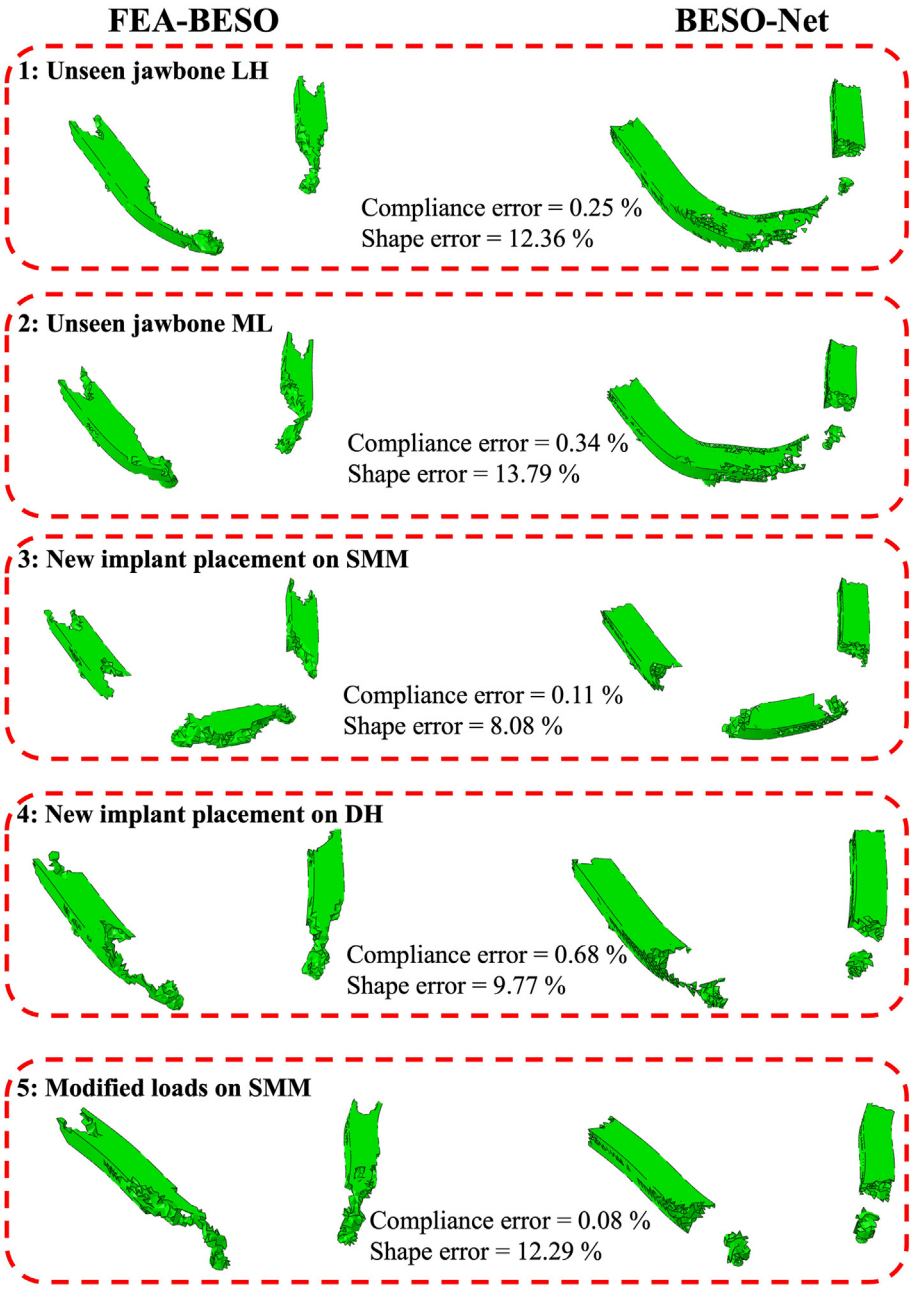

Figure 7 Comparison of optimal shapes obtained by FEA-BESO and BESO-Net. FEA: finite element analysis. BESO: bidirectional evolutionary structural optimization. SMM: standard mandibular model; ML: mesial-side low; DH: distal-side high.

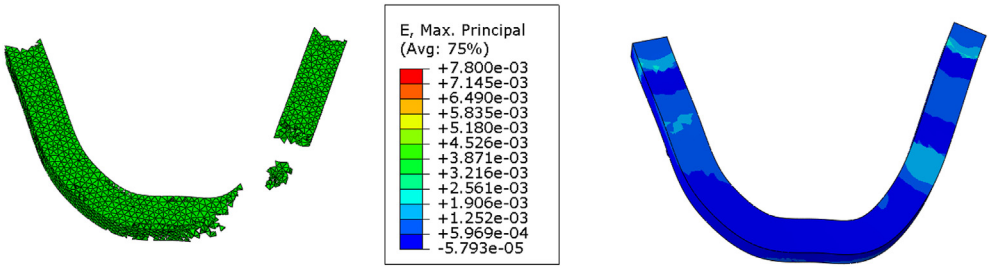

Figure 8 Optimal structure (generalization test case 2) predicted by BESO-Net and its strain contour obtained through post-analysis. BESO: bidirectional evolutionary structural optimization.

Table 6 Results of additional generalization test for changes in materials. Unit of compliance is N·mm.

Result item		Target volume						
		1	0.9	0.8	0.7	0.6	0.5	0.4
Compliance	FEA-BESO	265.2	265.2	265.3	265.5	265.7	266.1	266.7
	BESO-Net	265.2	265.9	265.3	265.6	265.9	266	266.6
	Error (%)	—	0.26	0	0.05	0.07	0.02	0.04
Shape difference	# of elements	0	3830	876	3428	3677	1933	1907
	Error (%)		17.41	3.98	15.58	16.71	8.79	8.67

FEA: finite element analysis. BESO: bidirectional evolutionary structural optimization.

simplification may lead to unrealistic stress and strain distributions at the bone-implant interface, but it would be valid as the focus of this study was on the strains that occur in the framework material.[36] Finally, the FEA models used in the study did not consider the actual forces exerted by the muscles during biting and chewing. Future research should aim to create more realistic FEA models by incorporating the jawbone geometry of actual patients and considering various load cases. This will enable a more accurate simulation of real-world scenarios.

The BESO-Net predicted an optimal structure that had compliance values closely matching the optimization results of FEA-BESO (Table 5), even when there were changes in loading conditions. We conducted additional tests to evaluate whether BESO-Net could maintain high prediction accuracy when new materials were considered for the framework and crown. We assigned zirconia for the framework and ceramic for the crown.[17] The results (Table 6) showed that the errors in compliance and shape were consistent with the previous test cases (Table 5), indicating that BESO-Net is capable of adapting to changes not only in jawbone, implant placement, and load but also in the material used.

In designing the All-on-4® prosthesis, it is important to consider various critical indicators in addition to the overall structural strength and material use for the framework. One of these indicators is the biomechanical performance of the prosthesis, which includes the displacement and stresses in the structure. It is also important to consider the mechanical behavior of bone, implants and their interfaces for patient comfort, potential side effects, or complications after treatment. To include these parameters in the optimization process, a combined objective function or new constraints can be added to the BESO process when generating data for training BESO-Net.

Since the optimized denture framework will be supported by the implants, it is necessary to develop another optimization process to determine the best implant placement that provides maximum support while minimizing the risk of mechanical damage. An FEA model can be established to simulate how the All-on-4® framework interacts with implants. By defining objective functions and implant design parameters, such as geometry and position, it is possible to optimize the implant placement for maximal stability and longevity of the All-on-4® system. Similar to the proposed method, an FEA-informed deep learning model can be developed to replace the time-consuming FEA and achieve real-time optimization for implant placement.

The development of the Python scripts that automated finite element modeling process can be a valuable tool for efficient data collection and future trainings. The process described in this paper demonstrated that the automation scripts developed are applicable to complex 3D models like the All-on-4® model investigated in this study. The method facilitated the inclusion of FEA in the shape data from all iterations in the BESO process, which enhances the accuracy of predicting the optimal framework design.

In conclusion, this study introduced an novel optimization approach, known as BESO-Net, for designing All-on-4® prosthesis. The approach integrated an FEA-based CNN with BESO to ensure optimal compliance of the framework structure while reducing material use. It has been proven that the approach can adapt to the changes in jawbone, implant, load, and material settings. The optimization time for BESO-Net was only 45 s, which was much less than the traditional topology optimization that required 6 h and 35 min. Future studies can include real patient data and additional FEA data fields to train the BESO-Net and conduct in-vitro experiments to validate its feasibility. A standard approach for verifying and validating numerical models used in medical device applications can be conducted to assess their credibility. By accurately defining the questions of interest and the context of use, in-vitro experiments can be designed to collect solid validation evidence for the applicability of the model.[37] These efforts could lead to significant advances in prosthesis design and improved clinical outcomes for patients.

Declaration of competing interest

The authors have no conflicts of interest in this study.

Acknowledgments

This study was supported by the grant from the National Science and Technology Council, Taiwan R.O.C (No. 111-2221-E-006-064).

References

1. Malo P, Rangert B, Nobre M. All-on-4 immediate-function concept with Branemark system implants for completely edentulous maxillae: a 1-year retrospective clinical study. *Clin Implant Dent Relat Res* 2005;7(Suppl 1):S88—94.

2. Liu T, Mu Z, Yu T, Wang C, Huang Y. Biomechanical comparison of implant inclinations and load times with the all-on-4 treatment concept: a three-dimensional finite element analysis. *Comput Methods Biomech Biomed Eng* 2019;22:585—94.
3. Geng JP, Tan KB, Liu GR. Application of finite element analysis in implant dentistry: a review of the literature. *J Prosthet Dent* 2001;85:585—98.
4. Gümrükçü Z, Korkmaz YT, Korkmaz FM. Biomechanical evaluation of implant-supported prosthesis with various tilting implant angles and bone types in atrophic maxilla: a finite element study. *Comput Biol Med* 2017;86:47—54.
5. Haroun F, Ozan O. Evaluation of stresses on implant, bone, and restorative materials caused by different opposing arch materials in hybrid prosthetic restorations using the all-on-4 technique. *Materials* 2021;14:4308.
6. Özdemir Doğan D, Polat NT, Polat S, Şeker E, Gül EB. Evaluation of "all-on-four" concept and alternative designs with 3D finite element analysis method. *Clin Implant Dent Relat Res* 2014;16:501—10.
7. Ahmadi A, Dörsam I, Stark H, Hersey S, Bourauel C, Keilig L. The all-on-4 concept in the maxilla-A biomechanical analysis involving high performance polymers. *J Biomed Mater Res B Appl Biomater* 2021;109:1698—705.
8. Wu AY, Hsu JT, Fuh LJ, Huang HL. Biomechanical effect of implant design on four implants supporting mandibular full-arch fixed dentures: in vitro test and finite element analysis. *J Formos Med Assoc* 2020;119:1514—23.
9. Moreira de Melo EJ Jr, Francischone CE. Three-dimensional finite element analysis of two angled narrow-diameter implant designs for an all-on-4 prosthesis. *J Prosthet Dent* 2020;124:477—84.
10. Ayali A, Altagar M, Ozan O, Kurtulmus-Yilmaz S. Biomechanical comparison of the all-on-4, M-4, and V-4 techniques in an atrophic maxilla: a 3D finite element analysis. *Comput Biol Med* 2020;123:103880.
11. Horita S, Sugiura T, Yamamoto K, Murakami K, Imai Y, Kirita T. Biomechanical analysis of immediately loaded implants according to the "all-on-four" concept. *J Prosthodont Res* 2017;61:123—32.
12. Almeida EO, Rocha EP, Freitas Júnior AC, et al. Tilted and short implants supporting fixed prosthesis in an atrophic maxilla: a 3D-FEA biomechanical evaluation. *Clin Implant Dent Relat Res* 2015;17(Suppl 1):e332—42.
13. de Sousa AA, Mattos BS. Finite element analysis of stability and functional stress with implant-supported maxillary obturator prostheses. *J Prosthet Dent* 2014;112:1578—84.
14. Cheng KJ, Liu YF, Wang R, et al. Topological optimization of 3D printed bone analog with PEKK for surgical mandibular reconstruction. *J Mech Behav Biomed Mater* 2020;107:103758.
15. Li CH, Wu CH, Lin CL. Design of a patient-specific mandible reconstruction implant with dental prosthesis for metal 3D printing using integrated weighted topology optimization and finite element analysis. *J Mech Behav Biomed Mater* 2020;105:103700.
16. Park J, Lee D, Sutradhar A. Topology optimization of fixed complete denture framework. *Int J Numer Method Biomed Eng* 2019;35:e3193.
17. Zhang Z, Chen J, Li E, Li W, Swain M, Li Q. Topological design of all-ceramic dental bridges for enhancing fracture resistance. *Int J Numer Method Biomed Eng* 2016;32:e02749.
18. Chanda S, Gupta S, Pratihar DK. A combined neural network and genetic algorithm based approach for optimally designed femoral implant having improved primary stability. *Appl Soft Comput* 2016;38:296—307.
19. Meo S, Zohoori A, Vahedi A. Optimal design of permanent magnet flux switching generator for wind applications via artificial neural network and multi-objective particle swarm optimization hybrid approach. *Energy Convers Manag* 2016;110:230—9.
20. Roy S, Dey S, Khutia N, Chowdhury AR, Datta S. Design of patient specific dental implant using FE analysis and computational intelligence techniques. *Appl Soft Comput* 2018;65:272—9.
21. Da Silva FB, Corso LL, Costa CA. Optimization of pedicle screw position using finite element method and neural networks. *J Braz Soc Mech Sci Eng* 2021;43:164.
22. Abueidda DW, Koric S, Sobh NA. Topology optimization of 2D structures with nonlinearities using deep learning. *Comput Struct* 2020;237:106283.
23. Black N, Najafi AR. Learning finite element convergence with the multi-fidelity graph neural network. *Comput Methods Appl Mech Eng* 2022;397:115120.
24. Lee S, Kim H, Lieu QX, Lee J. CNN-based image recognition for topology optimization. *Knowl Base Syst* 2020;198:105887.
25. Munoz D, Nadal E, Albelda J, Chinesta F, Rodenas JJ. Allying topology and shape optimization through machine learning algorithms. *Finite Elem Anal Des* 2022;204:103719.
26. Rade J, Balu A, Herron E, et al. Algorithmically-consistent deep learning frameworks for structural topology optimization. *Eng Appl Artif Intell* 2021;106:104483.
27. Shin J, Kim C. Bi-directional evolutionary 3D topology optimization with a deep neural network. *J Mech Sci Technol* 2022;36:3509—19.
28. Yan J, Qi Zhang, Qi Xu, et al. Deep learning driven real time topology optimisation based on initial stress learning. *Adv Eng Inf* 2022;51:104472.
29. Zheng S, He Z, Liu H. Generating three-dimensional structural topologies via a U-Net convolutional neural network. *Thin-Walled Struct* 2021;159:107263.
30. Xiang C, Wang D, Pan Y, Chen A, Zhou X, Zhang Y. Accelerated topology optimization design of 3D structures based on deep learning. *Struct Multidiscip Optim* 2022;65:99.
31. Huang X, Xie YM. Bi-directional evolutionary topology optimization of continuum structures with one or multiple materials. *Comput Mech* 2009;43:393—401.
32. Kumagai H, Suzuki T, Hamada T, Sondang P, Fujitani M, Nikawa H. Occlusal force distribution on the dental arch during various levels of clenching. *J Oral Rehabil* 1999;26:932—5.
33. Huang X, Xie YM. Bi-directional evolutionary topology optimization of continuum structures with one or multiple materials. *Comput Mech* 2009;43:393—401.
34. Zuo ZH, Xie YM. A simple and compact Python code for complex 3D topology optimization. *Adv Eng Software* 2015;85:1—11.
35. Szegedy C, Vanhoucke V, Ioffe S, Shlens J, Wojna Z. Rethinking the inception architecture for computer vision. *IEEE Comput Soc Conf Comput Vis Pattern Recogn* 2016:2818—26.
36. Verri FR, Cruz RS, de Souza Batista VE, et al. Can the modeling for simplification of a dental implant surface affect the accuracy of 3D finite element analysis? *Comput Methods Biomech Biomed Eng* 2016;19:1665—72.
37. Morrison TM, Hariharan P, Funkhouser CM, Afshari P, Goodin M, Horner M. Assessing computational model credibility using a risk-based framework: application to hemolysis in centrifugal blood pumps. *Am Soc Artif Intern Organs J* 2019;65:349—60.